Distortion of binoculars revisited: Does the sweet spot exist?

Holger Merlitz

Department of Physics and ITPA, Xiamen University, Xiamen 361005, China
(merlitz@gmx.de)

Received July 1, 2009; revised November 6, 2009; accepted November 11, 2009;
posted November 12, 2009 (Doc. ID 113648); published December 7, 2009

Sixty years ago, August Sonnefeld of Zeiss reported on observations with experimental telescopes. The goal of his investigation was to determine the ideal amount of distortion applied to optical instruments that are used in combination with the human eye. His studies were inconclusive and partially contradictory. We have picked up this problem once again, adopting a modern point of view about the human imaging process, and supported by computer graphics. Based on experiments with Helmholtz checkerboards, we argue that human imaging introduces a certain amount of barrel distortion, which has to be counterbalanced through the implementation of an equally strong pincushion distortion into the binocular design. We discuss in detail how this approach is capable of eliminating the globe effect of the panning binocular and how the residual pincushion distortion affects the image when the eye is pointing off-center. Our results support the binocular designer in optimizing his instrument for its intended mode of application, and may help binocular users and astronomers better understand their tools.

OCIS codes: 220.1000, 330.4060, 330.7321, 000.2850.

1. INTRODUCTION

In 1949, August Sonnefeld of Zeiss published a paper in the *Deutsche Optische Wochenschrift*, that would eventually change the design philosophy of contemporary binoculars [1]. Prior to 1950, the overwhelming majority of binoculars were constructed "free of distortion" [see Eq. (1) below for a definition], while subsequently a certain amount of pincushion distortion was added to the optical formula of handheld binoculars in order to improve their imaging properties. Currently, Nikon, in their latest catalog, suggests evaluating the apparent field of view once again according to the traditional tangent condition. Other binocular manufacturers seem ready to follow the trend to return to the design of "undistorted" binoculars. Hence, along with the 60th anniversary of Sonnefeld's memorable paper, it appears desirable to offer a reminder and search for the reasons that once initiated a paradigmatic change in binocular design.

Sonnefeld's studies had been triggered by frequently re-emerging complaints, in part from officers on the battlefields of both World Wars, concerning the imaging characteristics of contemporary handheld "Feldstecher." In order to eliminate its rectilinear distortion, a telescopic instrument was designed such that the ratio

$$\frac{\tan(a)}{\tan(A)} = m \quad \text{(tangent condition)} \tag{1}$$

remained constant all over the field of view [1]. Here, A stands for the true angle of the object with respect to the optical axis, a for the apparent angle of its image with respect to the center of field, and m for the (paraxial) magnification. This particular imaging equation, commonly denoted *tangent condition*, had already been introduced by Airy in 1827, and, since it was able to reproduce patterns on a flat surface undistorted over the entire field of view, it had been well established as the canonical design principle for distortion-free camera lenses. However, doubts remained whether or not the same design principle would be able to deliver an undistorted imaging of instruments that were used in combination with the human eye. In fact, binoculars designed after the tangent condition appeared to display a rather strange kind of distortion, which became particularly obvious whenever that binocular was used for panning. The moving image appeared to roll over a curved, convex surface. This phenomenon, henceforth denoted *globe effect*, seemed to be absent with the static image, but it miraculously reappeared with the moving image each time the binocular was panned. During the years of the First World War, Whitwell [2], Tscherning [3], and Weiss [4] had already speculated whether or not the *angle condition*

$$\frac{a}{A} = m \quad \text{(angle condition)} \tag{2}$$

would actually serve as a more suitable approach to optical instruments in combination with the human eye. In this spirit, Sonnefeld formulated the central question of his manuscript (freely translated by the author):

"The fundamental question is the following: For the application of the instrument in combination with the human eye, does the tangent or the angle condition represent the better approach to eliminate distortion?"

It is no surprise to find the community of leading optical designers assuming a critical position against the ideas of Whitwell and his supporters. Boegehold, Zeiss optician and former scholar of Abbe and assistant of von Rohr, rejected the angle condition in his 1921 paper,

clearly supporting the traditional tangent condition as being the only adequate approach to minimize distortion in binoculars [5].

Further complications were arising, because the imaging Eqs. (1) and (2) were just two examples of a huge variety of different schemes to transform the radial object angle A into its apparent angle a. In 1946, Slevogt, another member of the Zeiss design bureau, published a paper in which he analyzed the imaging process of the eye in considerable detail [6]. His approach was based on a much earlier work by Helmholtz [7], who had studied the distortion properties of curves under eye movements in accordance with Listing's law [8]. Slevogt's research resulted in the proposition that a binocular, if designed after yet another imaging equation,

$$\frac{\tan(a/2)}{\tan(A/2)} = m \text{ (circle condition)}, \tag{3}$$

would deliver a practically distortion-free image to the eye. Sonnefeld had subsequently denoted this equation as *circle condition*, because its characteristic property is to map small circles into circles over the entire field of view [1]. In his summary, Slevogt wrote (free translation by the author):

"We suggest denoting loupes and oculars as free of distortion if they satisfy the circle condition. Observations have to verify whether this definition is justified."

2. CONFUSING EXPERIMENTAL FINDINGS

In order to summarize the plethora of different imaging equations, we shall now introduce the more general expression

$$\frac{\tan(ka)}{\tan(kA)} = m, \tag{4}$$

featuring the distortion parameter k, which would be $k=1$ in case of the tangent condition, $k=0.5$ in case of the circle condition, and approach the limit $k \to 0$ in case of the angle condition.

In his 1949 paper, Sonnefeld reports on tests which he carried out with two self-made experimental telescopes of only $m=1.5\times$, but huge true angles of view of 90°. One of these two instruments was designed after the traditional tangent condition, Eq. (1), the other one after the angle condition, Eq. (2), as had previously been suggested by Whitwell and others. He reports [1]:

"I let 50 test persons, in disregard of their eye conditions, observe with these telescopes, and found that the overwhelming majority, and in particular the more experienced among them, regarded the one which matched the angle condition as almost free of distortion, while reporting an obvious barrel distortion with the other one which was made after the tangent condition."

However, his observations, carried out with another set of three self-made telescopes of 10×, were inconclusive:

"The observations did not lead to any clarification, since none of them delivered an image free of distortion. Although in particular the circle condition was satisfied to highest accuracy (i.e., in terms of the telescope design; this remark by the author), it clearly delivered a pincushion distortion, and even more so did the angle condition. An image almost free of distortion delivered that telescope, which actually failed to meet the tangent condition and instead exhibited a distortion characteristic between tangent and circle conditions."

Hence, the entire base of experimental data appeared to be inconsistent and confusing. In order to understand what Sonnefeld did in fact observe behind his oculars, we shall first return to Helmholtz's work of 1867 and take a closer look at the distortion properties of our visual imaging system.

3. HELMHOLTZ'S CHECKERBOARDS

In 1867, Helmholtz reported that a checkerboard pattern with a certain amount of pincushion distortion would appear undistorted when viewed from a specific, close distance [7]. The elimination of the pincushion distortion could be interpreted as the result of an additional perspective distortion that arises once the observer's eye approaches the distorted checkerboard pattern. Based on his theory of eye movement, Helmholtz's results were—as was later shown by Slevogt—consistent with the claim that the amount of pincushion distortion would have to satisfy the circle condition, Eq. (3), in order to deliver straight lines to the observer's eye. Recent studies have confirmed Helmholtz's findings in principle. However, it seems that the amount of pincushion distortion that is compensated by the visual system might be smaller than predicted by Helmholtz [9].

Let us now consider Helmholtz checkerboards with various degrees of distortion, Fig. 1, produced in the following way: Assuming a telescope with 10× power and 7° true field of view, Eq. (4) was applied using different val-

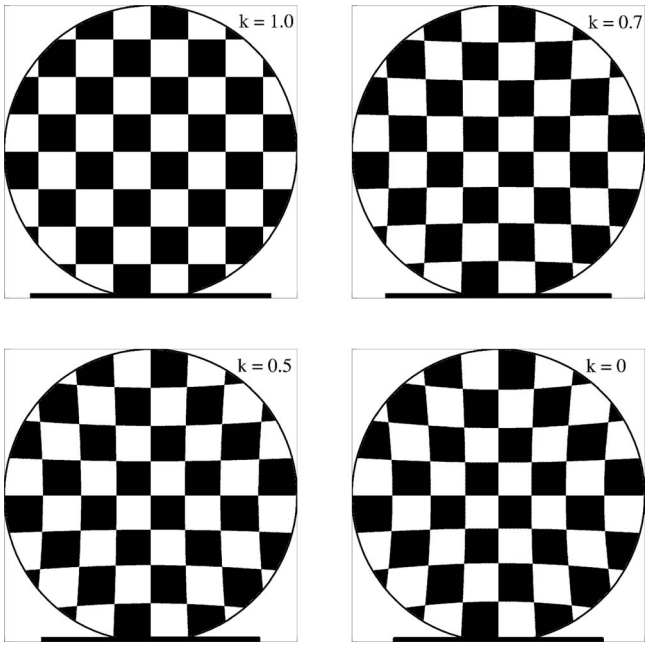

Fig. 1. Helmholtz checkerboards with various different amounts of pincushion distortion generated using Eq. (6). The distortion parameter k was defined in Eq. (4). To generate these images, an undistorted checkerboard pattern was imaged using telescopes with 10× and 7° true field of view.

ues of the distortion parameter k to image an undistorted checkerboard pattern. The imaging process is sketched in Fig. 2: A regular pattern on the wall (checkerboard) is mapped onto the image space of the binocular through Eq. (4). During this process, the object angle A of each point on the wall surface is transformed into the apparent angle a according to

$$a = (1/k)\arctan[m\tan(kA)]. \quad (5)$$

The apparent angular coordinates of all points of the wall surface define the properties of the image space, not to be confused with the visual space, which will be introduced in Eq. (8) below. Of course, the radial distance of any point to the center of field is proportional to $\tan(A)$ on the wall and $\tan(a)$ in image space. Therefore, the images in Fig. 1 display the radial distance of each image point computed as the tangent of the apparent angle, i.e.,

$$\tan(a) = \tan\{(1/k)\arctan[m\tan(kA)]\}. \quad (6)$$

If k equals unity (tangent condition), then

$$\tan(a) = m\tan(A), \quad (7)$$

i.e., a radial distance on the wall is linearly mapped into a radial distance in image space, and the image is free of distortion (upper left panel in Fig. 1). A reduction of k below unity introduces a pincushion distortion into the image space.

If we were dealing with cameras here, then this image space would coincide with the image plane of the lens and directly recorded by the photographic sensor, thereby finalizing the imaging process. Obviously, such a camera lens should be designed after the tangent condition ($k=1$) in order to generate undistorted images. The binocular, however, is an afocal system with a virtual image located in front of the observer. In order to reproduce the impression of the human vision behind the ocular, the image space has to be observed from a specific distance chosen such that its circular boundary appears under the same angle as the apparent angle of field of the binocular, which, in our case, amounts to roughly 70°. There are black bars plotted below the checkerboards in Fig. 1 that show the approximate distance from which the images have to be viewed using a single eye and strictly fixating

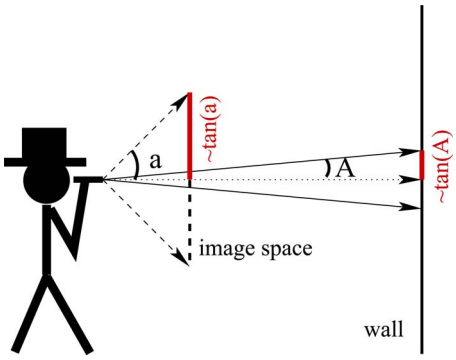

Fig. 2. (Color online) Flat surface (wall) is imaged into the image space by the binocular. During this process, the object angle A is transformed into the apparent angle a through Eq. (4). Any radial distance to the center of field corresponds to the tangent of that angle.

on the center of the image while analyzing the distortion properties of the checkerboard patterns.

The author has published full screen versions of these images and asked members of binocular and telescope discussion boards on the Internet to carry out this experiment [10]. The question was, which of these checkerboards would appear undistorted when viewed under the conditions mentioned above. Almost 30 test persons did participate, the majority of whom found that the checkerboard designed after $k=0.7$ came closest to delivering straight lines. A significant number of participants, among them a couple of amateur astronomers i.e., experienced visual observers, reported a slight barrel distortion with the $k=0.7$ checkerboard and, at the same time, a minor pincushion distortion with the $k=0.5$ checkerboard. This would indicate that the ideal amount of distortion that is exactly compensated by our visual system might be located somewhere between both examples.

These findings do partially coincide with the results of Oomes *et al.* [9]: In fact, the eye does superimpose a certain amount of barrel distortion on the image space, which eliminates a corresponding amount of its pincushion distortion. According to their studies, the quantity of this effect appears to be less than predicted by Helmholtz ($k=0.5$), but there exist large interindividual differences. Oomes *et al.* concluded that the exact amount of distortion compensated by the eye might be about half as strong as proposed by Helmholtz, which would correspond to a checkerboard of distortion $k\approx 0.8$. However, there are good reasons to believe that such an experiment might systematically underestimate the peripheral distortion of our visual system, and that the true amount of distortion might in fact be somewhat closer to the Slevogt/Helmholtz circle condition ($k=0.5$). We will discuss this matter again in Section 6, in which the situation of the rolling eye is studied in detail.

4. IMAGING EQUATIONS FOR THE HUMAN VISUAL SPACE

Based on the empirical findings of Section 3, we are now able to derive the imaging equations for our visual system. Here we have to implement the fact that a checkerboard (or, more generally, an image space) featuring a certain amount of pincushion distortion appears undistorted to the eye. This leads to our fundamental assumption:

Assumption: To each observer, there exists a certain, perhaps individually different, checkerboard that appears undistorted under the experimental conditions as described above.

As a consequence of this assumption, we are forced to introduce the following additional transformation that accounts for this empirical fact:

$$y = (1/l)\tan(la), \quad (8)$$

where y denotes the (perceived) radial distance of the image point with respect to the center of field, i.e., a radial distance in the transformed image space. We shall denote this transformed image space as *visual space*. The apparent angle a is given by Eq. (5). The empirical and possibly individually different parameter l describes the amount of distortion generated by the human visual imaging pro-

cess. Note that this transformation offers a parametric interpolation between the various classical schools: The assumption $l=1$ would imply that our eye is recording the image space without distortion (the classical Airy/Boegehold school), while $l\to 0$ would imply $y=a$ and support Whitwell with his angle condition. In Appendix A, we will show that the visual distortion parameter is actually equivalent to an intrinsic curvature of the visual space.

After inserting the apparent angle into Eq. (8) we obtain

$$y=(1/l)\tan\{(l/k)\arctan[m\,\tan(kA)]\}. \tag{9}$$

The special case $m=1$ delivers the imaging equation of the bare eye,

$$y=(1/l)\tan(lA), \tag{10}$$

in which the object angle A replaces the apparent angle a. If the distortion parameter of the binocular equals the distortion parameter of the eye, $k=l$, then Eq. (9) simplifies to

$$y=(m/l)\tan(lA). \tag{11}$$

Usually, binoculars offer magnifications that lead to rather small true fields of view, so that the object angles A do not exceed 5° and we safely approximate

$$y=(m/l)\tan(lA)\approx m\,\tan(A). \tag{12}$$

This transformation delivers an undistorted image of a wall pattern, because the radial distance $\tan(A)$ of the object on the wall surface is linearly mapped into the radial distance y of our visual space. In other words: The tangent condition ($k=1$), which generates undistorted images with a camera, has to be replaced with the condition $k=l$ in order to deliver undistorted images for visual instruments. The situation of low-power binoculars (e.g., opera glasses), which have large true fields of view, so that the above approximations are invalid, will be discussed later in Section 7.

The empirical findings of Section 3 imply that the distortion parameter of our eye is most likely located somewhere in the interval $l\in[0.6,0.8]$, perhaps with interindividual differences. For our illustrations and examples, we shall henceforth define a value of $l=0.6$, without loss of generality of the mathematical formalism. Figure 3 displays the images of the checkerboards (Fig. 1) as perceived by the observer when following the assumption $l=0.6$. It is also assumed that the observer is fixating his direction of view to the center of the checkerboard and viewing from the correct distance, so that the image appears under the same angle as the apparent angle of field of the binocular (≈70° in our example). The formerly undistorted image ($k=1$, tangent condition) now displays a significant barrel distortion, while the image formed with the angle condition ($k=0$) shows a pincushion distortion. Both intermediate cases ($k=0.5$, circle condition as proposed by Helmholtz) and $k=0.7$ are nearly undistorted, the former showing a very slight barrel and the latter a similarly small pincushion distortion. Naturally, the case $k=l=0.6$ would deliver an undistorted image here. Therefore, the important result of this section may be summarized as follows: While observing the image space as it is

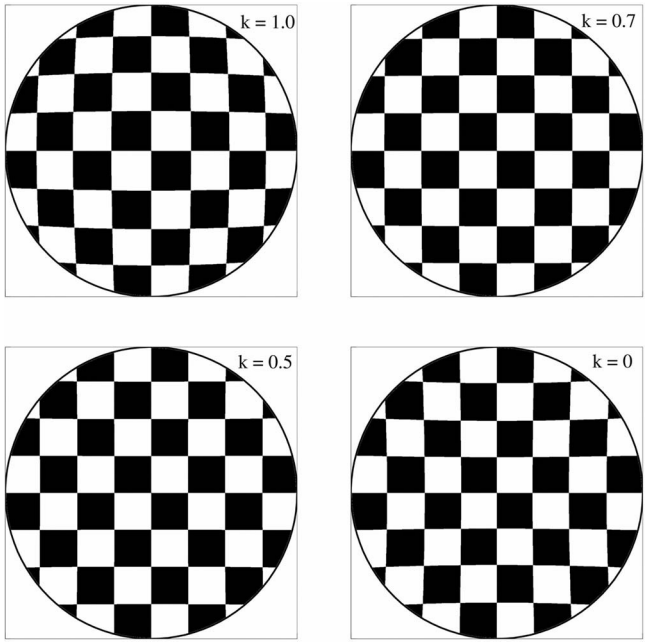

Fig. 3. Checkerboards of Fig. 1 in visual space, i.e., as they appear to the observer's eye when viewed close up and with the direction of view pointing to the center of the checkerboard. The transformation was carried out using the visual imaging Eq. (8) assuming a distortion parameter $l=0.6$.

generated by the binocular, the human visual imaging process adds a certain additional amount of barrel distortion, which has to be compensated for through an equally strong pincushion distortion along with the binocular design in order to deliver an undistorted image to the eye (i.e., in visual space).

5. CHARACTERISTIC DRIFT RATIO AND GLOBE EFFECT

The previously discussed distortions also affect the image properties of the panning binocular. Whenever a binocular is used for surveillance applications, the observer has to deal with a moving image, and it was the peculiar behavior of the moving image that triggered the redesign of binoculars sixty years ago after a series of scientific discussions among the team of Zeiss engineers.

Whenever a binocular is panning, the angle of each object around us turns into a variable of time. For the case of simplicity, let us discuss the trajectory of a distant object (e.g., a star), which, during panning, enters the field of view at the edge, then passes through the center, and finally exits at the opposite side of the field. We can evaluate the radial velocity of the object inside the visual space as

$$\dot{y}=\frac{m\dot{A}\cos^{-2}(kA)}{\cos^2\{(l/k)\arctan[m\,\tan(kA)]\}[1+m^2\tan^2(kA)]}, \tag{13}$$

which, at the center of field, simplifies to

$$\dot{y}(0) = m\dot{A}. \tag{14}$$

$\dot{A}$ is the time derivative of the object angle, i.e. the angular velocity of the panning binocular. We shall define the *characteristic drift ratio*

$$\Gamma \equiv \frac{\dot{y}(A)}{\dot{y}(0)}, \tag{15}$$

which defines the radial velocity of the image point as a function of the object angle, scaled with its velocity at the center of field, yielding

$$\Gamma = \frac{\cos^{-2}(kA)}{\cos^2\{(l/k)\arctan[m\,\tan(kA)]\}[1 + m^2\tan^2(kA)]}. \tag{16}$$

This quantity is plotted in Fig. 4, again assuming a visual distortion parameter of $l=0.6$. For the case $k=l$, the drift of the object is practically constant, because in this case Eq. (16) simplifies to

$$\Gamma = \frac{1}{\cos^2(lA)}, \tag{17}$$

and since the field of view of the binocular, and hence A, remain small, this term approximately equals unity all over the field of view. This implies a constant velocity of the object while passing through the field of view and hence avoids the emergence of any spurious image curvature. Once the distortion of the binocular is reduced, i.e., k is driven to higher values toward unity, the drift ratio drops toward the edges of the field. This slowdown of the object's velocity is consequence of the barrel distortion in the visual space and generates the impression of an image rolling over a convex surface—the globe effect, which has been reported to cause symptoms of motion sickness to some observers while panning. The author has presented a couple of computer animations on his web page that demonstrate the impact of these phenomena with the panning binocular [10].

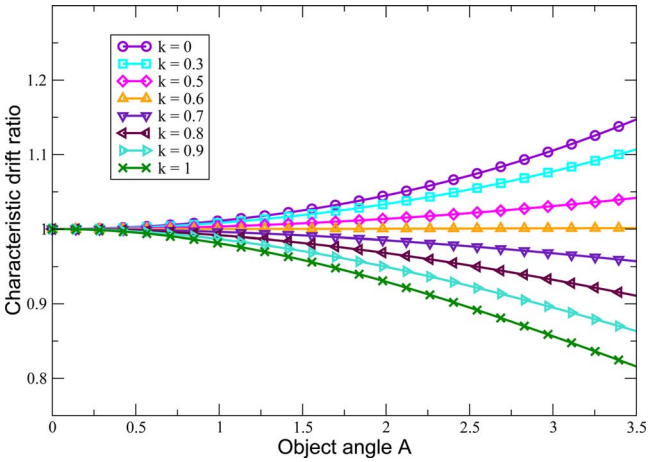

Fig. 4. (Color online) Characteristic drift ratio Γ, Eq. (16), for different degrees of distortion k as a function of the object angle A. Here, we assume a binocular with $m=10\times$ and 7° true field of view. The visual distortion parameter was assumed to be $l=0.6$.

The opposite effect arises when the pincushion distortion is increased via reduction of k below the critical value $k=l$: Now, the image points speed up toward the edges of field, because there exists a residual pincushion distortion inside the visual space. This generates the impression of an image rolling over a concave surface, i.e., objects seem to move away from the observer when approaching the central region of the field (the reader may consult the literature on optical flow here, e.g., [11]). In this context, it is interesting to discuss the case of the angle condition $k \to 0$. Here, Eq. (16) simplifies to

$$\Gamma = \frac{1}{\cos^2(lmA)}, \tag{18}$$

which, through Eq. (2), delivers

$$\Gamma = \frac{1}{\cos^2(la)}. \tag{19}$$

This equals the characteristic drift ratio of the bare eye,

$$\Gamma = \frac{1}{\cos^2(lA)}, \tag{20}$$

in which the apparent angle a is replaced with the true angle A. One might therefore argue that the choice of the angle condition ($k=0$) would deliver the most natural panning behavior for any binocular, because it would offer the same velocity characteristics as does the bare eye while turning the head. However, there are a couple of serious objections to such an approach. As discussed in Appendix A, the intrinsic curvature of the visual space generates a certain amount of perceived curvature of the world when observed with the bare eye. The functional identity of both Eqs. (19) and (20) implies that the apparent angle 'a' through the telescope behaves exactly as an equally large true angle 'A' observed with the bare eye. Applying this to the sky, we now perceive the same image curvature through our binocular (which is actually imaging a small, practically flat surface element of the sky) as we do with the bare eye (which covers a large, curved surface element of the sky). This would perhaps be suitable for handheld astronomical instruments, since while panning, stars display a motion along a concave surface just as they do when observed with the bare eye. However, the binocular now imposes the same amount of curvature to any other flat surface element, e.g., the wall of a house, which shows up as a residual pincushion distortion in Fig. 3 (lower right), making the binocular less suitable for terrestrial observation.

6. THE ROLLING EYE

The situation turns more complex once the direction of view no longer coincides with the optical axis of the instrument. If the observer is pointing his direction of view away from the center of the field, then the image space is seen from an angle and additional perspective distortions are emerging. Figure 5 displays what is happening to the image of a regular wall pattern once the observer is fixating a point 20° (measured in apparent angle) below the

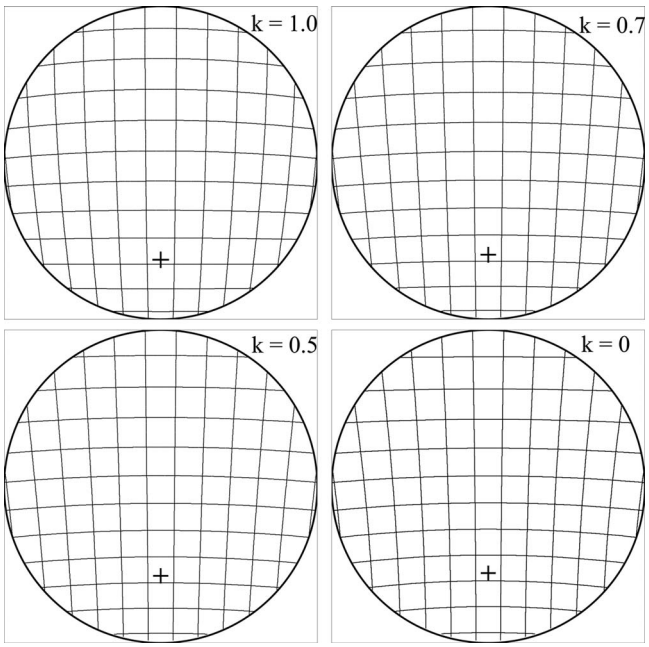

Fig. 5. Visual space and the rolling eye. Here, the direction of view (cross) is offset 20° below the center of field. A visual distortion parameter of $l=0.6$ was assumed.

center of field. Again, a 10× binocular with 7° true field of view is assumed and a visual distortion parameter of $l=0.6$.

When interpreting these images, it is important to realize that the observer's impression about the imaging characteristics of his binocular is strongly influenced by the amount of distortion he perceives near the direction of view, where the visual acuity is at its maximum. Figure 5 demonstrates that in the case of the tangent condition ($k=1$), lines appear locally straight near the direction of view. Our overall impression therefore is that of an undistorted image, despite the fact that there exists a global barrel distortion of the image. The latter becomes evident rather with the panning binocular, as discussed in Section 5, when the image is rolling as a global entity in front of the eye. As soon as the distortion parameter k is reduced below unity, an inward curvature of the line emerges near the direction of view, delivering the impression of a distorted image. This is the consequence of the intrinsic pincushion distortion of the image space, which, as a result of the broken rotational symmetry, can no longer be compensated for by the transformation Eq. (8). Hence, for off-center observations, the condition $k=l$ no longer delivers undistorted images to the eye. For $k=0.7$, the perceived distortion is still very weak and hardly noticeable to the user. The circle condition ($k=0.5$) and in particular the angle condition ($k=0$), however, deliver a significantly stronger pincushion distortion.

The results of this section are of relevance when interpreting the visual experiment with checkerboards of Section 3. During these experiments, the test persons were asked to keep their eyes fixated at the center of the checkerboard, in order to judge the curvature of the lines exclusively through peripheral observation. However, this fixation was neither enforced nor controlled by the experimental setup, and eye movements might have occurred unintentionally. In this case, the residual pincushion distortion would show up, and the observer would tend to select another checkerboard with a higher k value as his personal "undistorted" candidate. Hence the results of such a test might potentially be biased toward higher values of k, i.e., weaker pincushion distortion.

7. LOW-POWER BINOCULARS

If the binocular has a low magnification m, then its true field of view is often very large. In this case, the approximation made in Eq. (12) no longer remains valid, and the image displays a residual distortion for the case $k=l$ even when the observer is fixating its central region. Since for any $l<1$ we have

$$\frac{l^{-1}\tan(lA)}{\tan(A)}<1, \tag{21}$$

a regular wall pattern is being contracted at large object angles A, so that the image picks up an additional barrel distortion. Equation (9) suggests that the choice of a distortion $k<l$ might be used to increase the ratio l/k, and at the same time drive the term $\tan(kA)$ toward the linear regime in order to counterbalance that barrel distortion. Figure 6 displays the distortions that correspond to Sonnefeld's experimental telescope with $m=1.5$ and huge true angle of field of 90°. The tangent condition ($k=1$) does in fact generate a very strong barrel distortion, which is not fully eliminated by the pincushion distortion imposed in the $k=0.7$ case or the circle condition ($k=0.5$). Only the angle condition ($k=0$) nearly eliminates the barrel distortion of this telescope. Hence, Sonnefeld's observations as reported in Section 2, were in fact correct: For such a telescope, the angle condition delivers an image almost free of

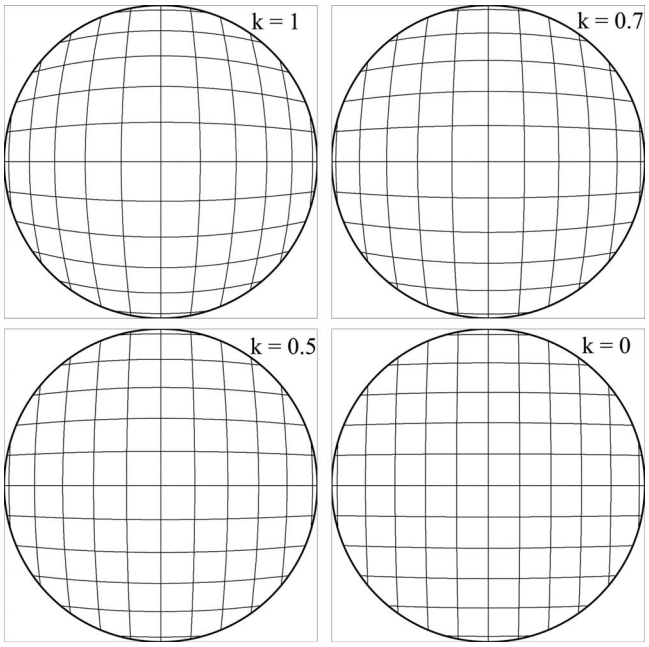

Fig. 6. Distortion properties of Sonnefeld's experimental telescope with low power $m=1.5$ and huge true field of view of 90° as it is perceived in visual space. Only the angle condition offers an almost undistorted image. A visual distortion parameter $l=0.6$ was assumed.

distortion, while the tangent condition generates a clearly visible barrel distortion.

Figure 7 displays the distortion parameter k, derived numerically, that would be required to fully eliminate the distortion of the image in visual space as a function of the magnification. For these calculations, a constant apparent field of view equal to Sonnefeld's telescope was assumed with the visual distortion parameter of $l=0.6$. Obviously, for magnifications usually applied to handheld binoculars, the condition $k=l$ offers a good choice to eliminate the barrel distortion. Perhaps opera glasses with magnifications below $m\approx 4$ might be designed with an additional pincushion distortion ($k<l$) to account for the residual barrel distortion of such a wide (true) angle device. However, the same pincushion distortion would then turn annoying once the instrument were used with the rolling eye, as was discussed in Section 6. Therefore, it is not advisable to make use of the option $k<l$ even in case of low-power instruments, but to stick to the condition $k\approx l$ instead.

8. SUMMARY

An optical instrument that is used in combination with the eye does not behave like a camera. Instead, human visual imaging imposes an additional transformation of the image generated by the instrument. This transformation may be approximated by Eq. (8), featuring the visual distortion l, which may equivalently be interpreted as a curvature of our visual space (Appendix A). The exact value of this parameter is unknown and probably shows inter-individual differences, but the tests carried out by Oomes [9] and by the author (Section 3) would suggest a range of $l\in[0.6,0.8]$ valid for most individuals, with the larger values of l possibly being affected by systematic errors, as discussed in Section 6. Within this work, we have consistently assumed a value of $l=0.6$, though the conclusions drawn from our analysis remain valid for any other value of l.

The choice of the ideal amount of distortion for a binocular, i.e., the value of k in Eq. (4), is a difficult one and necessarily involves compromises. Since binocular observations, similar to bare eye observations, do involve the imaging of the rolling eye, one might be tempted to choose a distortion close to the tangent condition (1), because in this case straight contours of objects are locally imaged as straight lines (Section 6 and Fig. 5). However, such a binocular would generate a globe effect that would significantly affect the imaging characteristics of the panning binocular (Section 5 and Fig. 4). The globe effect is eliminated once the condition $k=l$ is satisfied, i.e., the curvature of the image space matches the curvature of the visual space. The same condition also guarantees an undistorted image if, and only if, the observer's direction of view coincides with the optical axis, i.e., he is fixating the center of field. Low-power binoculars, e.g., opera glasses, would ask for the implementation of $k<l$ to achieve the latter effect, but there are good reasons to refrain from that option and stick to the condition $k\approx l$ instead (Section 7).

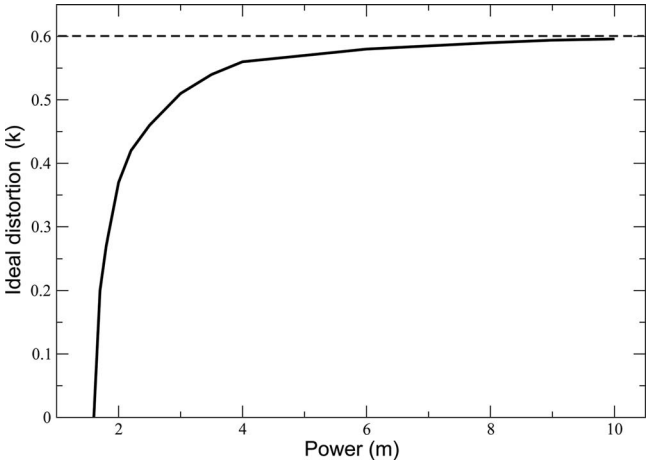

Fig. 7. Distortion parameter k that would be required to fully eliminate the barrel distortion in visual space as a function of the power m and assuming a visual distortion of $l=0.6$.

From a historical point of view, Sonnefeld was correct to demand the implementation of pincushion distortion into handheld binoculars, though he overestimated the quantity of distortion when he suggested the angle condition ($k=0$). Slevogt's suggestion to implement the circle condition ($k=0.5$) was based on Helmholtz's idea and appears to be close to the ideal solution. The sweet spot is most likely located between the circle and the tangent condition, a claim that coincides with the results already reported by Sonnefeld when he did his observations with experimental telescopes of 10× power. However, he was confused by his own findings, since similar experiments with his 1.5× power telescope were pointing toward the angle condition instead. We have solved this puzzle in Section 7, while showing that the angle condition is able to deliver undistorted images in the case of low-power telescopes only. It therefore appears that the ideal amount of distortion for handheld binoculars should be chosen between $k=0.6$ and $k=0.8$, a choice that would leave both the globe effect and the pincushion distortion (with the rolling eye) on a reasonably low level. Binocular designers might also considering building oculars that would enable the user to modify the amount of distortion. In this way, the observer would be able to optimize the distortion characteristics of his instrument according to his own individual preferences and the particular mode of application.

APPENDIX A: CURVATURE OF THE VISUAL SPACE

The transformation equation for the bare eye, Eq. (10), generates a certain amount of barrel distortion, depending on the value of the distortion parameter l. There has been discussion about the origin of this distortion, which might be the result of a combination of different phenomena [12]. Here we want to interpret this distortion as an intrinsic curvature of the visual space, because this approach perfectly harmonizes with the experience of the globe effect (Section 5). In order to analyze this curvature, we first note that the transformation generated by Eq. (10) is symmetric about the center of field, so that it is suf-

ficient to reduce its analysis to a two-dimensional cross section of the visual space, delivering curves in the x-z plane (Fig. 8).

A line element along such a curve is found from Eq. (10) through differentiation:

$$dy = \frac{d}{dA}\left(\frac{1}{l}\tan(lA)\right)dA = \frac{dA}{\cos^2(lA)}. \tag{A1}$$

When defining the radius vector $\rho(A)$ centered at (0, 1) and generating a parameterization of the curve as shown in Fig. 8, then the following triangle equation holds for infinitesimal increments of the angle A:

$$(dy)^2 = \rho^2(dA)^2 + (d\rho)^2. \tag{A2}$$

This delivers the following differential equation for the magnitude of $\rho(A)$:

$$\frac{d|\rho|}{dA} = \pm\sqrt{\frac{1}{\cos^4(lA)} - \rho^2}, \tag{A3}$$

where we consider the positive branch only. For the case $l=1$ and the boundary condition $|\rho(A=0)|=1$ we easily obtain the solution $|\rho(A)|=\cos^{-1}(A)$, which implies that the tip of the radius vector moves along the x axis: The resulting curve is flat and the visual space Euclidean (dashed curve in Fig. 8). For $l=0$ we obtain $d|\rho|=0$ regardless of the angle A, i.e., the vector has a constant length and describes a circle. The visual space is then spherical (dotted curve). Both limit cases are easily verified using Eq. (10), which would simplify to $y=A$ at the limit $l\to 0$. Our experiment of Section 3 implies a parameter value of l somewhere between both extremes. Figure 8 displays the curvature of the visual space corresponding to $l=0.6$ (solid curve, numerical solution), which is smaller than that of a circle, but far from being flat like the Euclidean space.

The distortions generated by the transformation formula Eq. (10) may thus be interpreted as an intrinsic curvature of our visual space. In the same way it can be shown that the distortion parameter k implemented into binocular design is related to a curvature of the resulting image space, which is flat only in the case of $k=1$. In this sense, the matching of both parameters, $k=l$, means nothing else but matching both curvatures, which is the key to the elimination of the globe effect of Section 5.

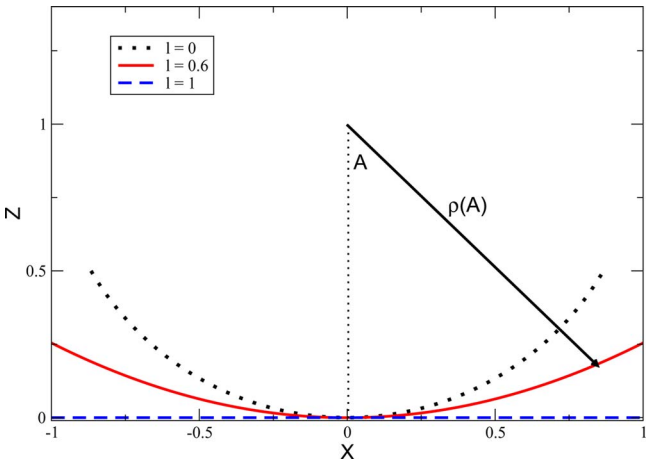

Fig. 8. (Color online) Curvature of the visual space as a function of the visual distortion parameter l. For $l=0$, the space is spherical, for $l=1$ it is flat (Euclidean). The curves are parameterized by the radius vector $\rho(A)$.

Finally, we would not assume that a model as simple as that might be able to offer a complete description of human vision. This model was designed to be consistent with the checkerboard experiment, and it also explains phenomena such as the globe effect and Sonnefeld's observations with low-power telescopes. Beyond that, we shall refer to Mark Wagner [13]:

"In fact, the geometry that best describes visual space changes as a function of experimental conditions, stimulus layout, observer attitude, and the passage of time (p. 11). The human mind is flexible enough and the world provides enough variation that no single geometry can fully encompass human visual experience" (p. 223).

ACKNOWLEDGMENTS

The author thanks the members of www.astronomie.de and www.juelich-bonn.com for participating in the experiment with Helmholtz's checkerboards. He is grateful for countless fruitful discussions with Walter E. Schön and Albrecht Köhler.

REFERENCES

1. A. Sonnefeld, "Über die Verzeichnung bei optischen Instrumenten, die in Verbindung mit dem rollenden Auge gebraucht werden," Deutsche Optische Wochenschrift **13**, 97–99 (1949).
2. A. Whitwell, "On the sine, the tangent and the angle conditions," The Opt. **48**, 149–153 (1914).
3. H. Tscherning, "Moyens de controle de verres de lunettes et de systèmes optiques en général," Kgl. Danske Vid. Selsk. Math. Fys. Medd. **9**, 3–29 (1918).
4. E. Weiss, "Analytische Darstellung des Brillenproblems für sphärische Einzellinsen," Central Ztg. Optik Mechanik **41**, 321–325 (1920).
5. H. Boegehold, "Treue Darstellung und Verzeichnung bei optischen Instrumenten," Naturwiss. **9**, 273–280 (1921).
6. H. Slevogt, "Zur Definition der Verzeichnung bei optischen Instrumenten für den subjektiven Gebrauch," Optik (Stuttgart) **1**, 358–367 (1946).
7. H. v. Helmholtz, *Handbuch der physiologischen Optik*, Vol. 3, v. Kries, ed. (Hamburg und Leibzig, 1910).
8. A. Barre and A. Flocon, *Curvilinear Perspective*, R. Hansen, trans. and ed. (Univ. California Press, 1987).
9. A. H. J. Oomes, J. J. Koenderink, A. J. Doorn, and H. de Ridder, "What are the uncurved lines in our visual field? A fresh look at Helmholtz's checkerboard," Perception **38**, 1284–1294 (2009).
10. www.holgermerlitz. de/globe/distortion.html.
11. I. P. Howard and B. J. Rogers, *Binocular Vision and Stereopsis* (Oxford Univ. Press, 1995).
12. B. Rogers and K. Brecher, "Straight lines, 'uncurved lines', and Helmholtz's 'great circles on the celestial sphere'," Perception **36**, 1275–1289 (2007).
13. M. Wagner, *The Geometries of Visual Space* (Erlbaum, 2006).